Coupled Systems Mechanics, *Vol. 15, No. 3 (2026) 227-241*
https://doi.org/10.12989/csm.2026.15.3.227

Flexural-torsional behavior of channel steel beams considering large deformation and additional torque: theory and experiment

Yipei Zeng[1], Fuli Liu[1], Xianhui Yi[1], Langhong Tang[1], Songqiang Li[1], Xiao Li[1], Yong Cai*[2]

[1]*China Construction Fifth Bureau Installation Engineering Co., Ltd, Shenzhen 410004, China*
[2]*School of Civil Engineering, Central South University, Changsha 410075, China*

(Received March 23, 2026, Revised June 15, 2026, Accepted June 19, 2026)

Abstract. This study investigates the flexural-torsional behavior of channel steel beams used in prefabricated hanger systems under large deformation. A geometrically nonlinear analytical model is developed based on Vlasov thin-walled beam theory and Green-Lagrange strain, incorporating centroid migration and the resulting additional torsional moment. The governing equations are derived using the variational principle and solved by the Galerkin method. Experimental tests on two representative channel sections subjected to mid-span concentrated loading are conducted for validation. Good agreement between theoretical predictions and experimental results confirms the accuracy of the proposed model. Parametric analysis shows that geometric nonlinearity and flexural-torsional coupling become increasingly significant with increasing span. The nonlinear deformation amplification factor increases from 1.02 to 1.38, while the flexural-torsional contribution rises from 2.8% to 23.7% as the span increases from 500 mm to 3000 mm. The proposed model provides a practical basis for the design of long-span prefabricated hanger systems.

Keywords: additional torsional moment; channel steel beam; flexural-torsional coupling; geometric nonlinearity; prefabricated hanger system

1. Introduction

Prefabricated and modular construction technologies have been increasingly adopted in contemporary civil engineering owing to their advantages in construction efficiency, quality control, sustainability, and reduced on-site labor demand [1]. As an important component of building service infrastructure, prefabricated support and hanger systems are extensively employed to support mechanical, electrical, and plumbing pipelines in industrial and commercial buildings [2]. The structural safety and serviceability of these systems directly affect the long-term performance of building facilities. Among various structural members, channel steel beams are widely used as primary load-carrying components because of their favorable manufacturability and assembly efficiency [3]. However, the open thin-walled geometry of channel sections generally results in relatively low torsional stiffness and a distinct separation between the centroid and shear

*Corresponding author, Professor, E-mail: glut436166@163.com

Copyright © 2026 Techno-Press
http://www.techno-press.org/csm/5
ISSN: 2234-2184 (Print), 2234-2192 (Online)

center, making them susceptible to coupled bending-torsion deformation under transverse loading [4]. With the increasing demand for long-span and lightweight support systems, understanding the flexural-torsional response of channel steel beams has become an important issue for the safe design and assessment of prefabricated hanger structures [5].

Extensive studies have been conducted on the mechanical behavior, stability, and design of cold-formed steel channel members. Experimental investigations demonstrated that the cross-sectional configuration significantly influences the buckling behavior and load-carrying capacity of channel and sigma beam-columns subjected to combined loading conditions [6]. Further studies revealed that sigma sections generally exhibit improved buckling resistance compared with conventional lipped channel sections because of enhanced web stiffness [7]. To improve design accuracy, advanced methods such as the Continuous Strength Method and the Direct Strength Method have been developed and applied to channel columns and beams exhibiting distortional buckling behavior [8]. Data-driven approaches have also been introduced to predict the strength of cold-formed steel beam-columns, providing alternative solutions to traditional code-based design procedures [9].

For perforated channel members frequently used in engineering applications, experimental and analytical investigations demonstrated that web openings substantially affect local, distortional, and interactive buckling responses, thereby requiring modifications to existing design formulations [10]. Similar conclusions were reported in studies focusing on web-perforated channel columns, where the presence of openings altered failure mechanisms and reduced structural resistance [11]. The influence of cross-sectional configuration on flexural performance has also been examined for laminated channel beams and non-symmetric channel sections under bending actions [12]. Investigations on channel members subjected to elevated temperatures further highlighted the complexity of distortional buckling behavior and the limitations of existing design approaches [13]. In addition, the structural performance of prefabricated steel systems has attracted increasing attention, including assembly-oriented beam-column connections [14], high-strength channel members [15], interlocking joints in support and suspension systems [16], earthquake-resilient channel beam-column joints [17], machine-learning-based strength prediction of channel beams with web openings [18], and axial performance of interlocking joints used in prefabricated hanger systems [19].

Although considerable progress has been achieved in understanding the buckling resistance, strength prediction, and connection behavior of channel steel members, several important issues remain unresolved. Existing studies primarily focus on ultimate strength, buckling modes, or design optimization, whereas the nonlinear deformation process associated with flexural-torsional coupling has received comparatively limited attention. In particular, most available analytical formulations are developed under small-deformation assumptions and do not explicitly consider the influence of centroid migration induced by torsional rotation. For open thin-walled channel sections, the displacement of the centroid during deformation may alter the load eccentricity and generate additional torsional actions, leading to stronger interaction between bending and torsion. Furthermore, experimental evidence specifically addressing the large-deformation flexural-torsional behavior of channel steel beams employed in prefabricated hanger systems remains scarce. Consequently, a comprehensive theoretical framework capable of capturing geometric nonlinearity, torsional deformation, and deformation-induced additional torque is still lacking.

To address these limitations, this study develops a geometrically nonlinear analytical model for channel steel beams based on Vlasov thin-walled beam theory and Green-Lagrange strain theory. The proposed formulation explicitly incorporates centroid migration and the associated additional torsional moment into the flexural-torsional coupling analysis. The governing equations are derived using the variational principle and solved through the Galerkin method. Experimental tests on representative channel steel sections subjected to mid-span concentrated loading are conducted to validate the theoretical predictions. Subsequently, a parametric investigation is performed to evaluate the influence of beam span on nonlinear deformation characteristics and flexural-torsional interaction. The remainder of this paper is organized as follows. Section 2 presents the theoretical formulation and nonlinear governing equations. Section 3 describes the experimental program and model validation. Section 4 discusses the parametric analysis results. Finally, the main conclusions are summarized in the last section.

2. Theoretical model

2.1 Kinematic description of the channel steel beam

Prefabricated channel steel hangers consist of two vertical columns and a horizontal channel beam. Under service loads, the horizontal beam may experience significant bending deformation accompanied by flexural-torsional coupling due to the eccentricity between the centroid and shear centre of the open section. To establish a geometrically nonlinear model based on Vlasov thin-walled beam theory, the following assumptions are adopted:

(1) The cross-section remains rigid in its own plane during deformation, while warping deformation of the open section is permitted.

(2) The material is assumed to remain linearly elastic throughout the loading process.

(3) Large displacement effects are considered through Green-Lagrange strain, whereas the torsional rotation remains moderate.

(4) The centroid migration induced by torsional deformation is taken into account, and the resulting additional torsional moment contributes to the flexural-torsional coupling behavior.

A Cartesian coordinate system (x, y, z) in Fig. 1 is established, where the x-axis coincides with the beam longitudinal axis, while the y- and z-axes correspond to the principal axes of the cross-

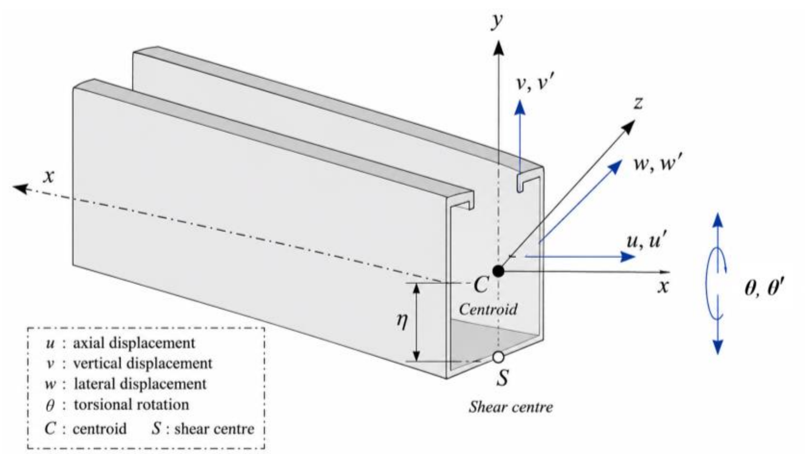

Figure 1. Kinematic description and displacement components of the channel steel beam

section. The displacement components of the centroid are denoted by $u(x)$, $v(x)$, and $w(x)$, representing the axial, vertical, and lateral displacements, respectively. The twist angle of the cross-section is denoted by $\theta(x)$. According to Vlasov thin-walled beam theory [20], the displacement field of an arbitrary point in the cross-section can be expressed as:

$$U(x,y,z) = u(x) - yv'(x) - zw'(x) - \omega\Phi'(x) \tag{1}$$

$$V(x,y,z) = v(x) - z\Phi(x) \tag{2}$$

$$W(x,y,z) = w(x) + (y-\eta)\Phi(x) \tag{3}$$

where ω is the sectorial coordinate associated with warping deformation. The prime symbol ($''$) denotes the derivative with respect to x. The above displacement assumptions simultaneously account for bending deformation, Saint-Venant torsion, and restrained warping effects of thin-walled open sections.

2.2 Centroid migration induced by torsion

For monosymmetric channel sections, the centroid C and shear centre S are separated by a distance η. Under torsional deformation, the centroid no longer remains at its original position. Following the geometric relationship proposed for open thin-walled members, the coordinates of the deformed centroid become:

$$v_c = v + \eta\theta \tag{4}$$

$$w_c = w \tag{5}$$

where η denotes the distance between the centroid and the shear centre. The above expressions indicate that torsional rotation produces an additional transverse displacement of the centroid. Although this effect is usually neglected in small-deformation analyses, it becomes increasingly significant for long-span channel steel beams undergoing large deformation.

In conventional flexural-torsional coupling theory, external loads are assumed to act at fixed locations. However, after torsional deformation occurs, the migration of the centroid modifies the actual load eccentricity. Consequently, an additional torsional moment is generated. The total torsional moment acting on the cross-section can therefore be written as:

$$\bar{M}_t = M_t + M_a \tag{6}$$

where M_t is the externally applied torsional moment and M_a is the additional torsional moment induced by centroid migration.

Based on equilibrium considerations, the additional torsional moment is calculated as:

$$M_a = \eta EI_z w'''' + \eta\theta EI_y v'''' \tag{7}$$

The first term represents the additional torsional action induced by lateral bending curvature, whereas the second term reflects the amplification effect associated with the rotation of the eccentric load path during twisting deformation. This mechanism constitutes a secondary geometric nonlinear effect and is one of the primary sources of flexural-torsional interaction in channel steel hanger beams.

Accordingly,

$$\bar{M}_t = M_t + \eta E I_z w'''' + \eta\theta E I_y v'''' \tag{8}$$

2.3 Green-Lagrange strain under large deformation

To account for geometric nonlinearity, the Green-Lagrange strain tensor [21] is adopted. The axial normal strain can be expressed as:

$$\varepsilon_x = \varepsilon_x^L + \varepsilon_x^N \tag{9}$$

where $\varepsilon_x{}^L$ is the linear normal strain caused by small deformation, defined as

$$\varepsilon_x^L = \frac{\partial U(x,y,z)}{\partial x} = u'(x) - yv''(x) - zw''(x) - \omega\Phi''(x) \tag{10}$$

and the nonlinear component is:

$$\begin{aligned}\varepsilon_x^N &= \frac{1}{2}\left[\left(\frac{\partial U(x,y,z)}{\partial x}\right)^2 + \left(\frac{\partial V(x,y,z)}{\partial x}\right)^2 + \left(\frac{\partial W(x,y,z)}{\partial x}\right)^2\right] \\ &= \frac{1}{2}\left\{\begin{matrix}\left[u'(x) - yv''(x) - zw''(x) - \omega\Phi''(x)\right]^2 \\ +\left[v'(x) - z\Phi'(x)\right]^2 + \left[w'(x) + (y-\eta)\Phi'(x)\right]^2\end{matrix}\right\}\end{aligned} \tag{11}$$

Assuming linear elastic material behavior, the normal and shear stresses are given by

$$\sigma_x = E\varepsilon_x, \tau = G\gamma \tag{12}$$

where E and G denote the elastic modulus and shear modulus, respectively.

The Saint-Venant torsional shear strain γ is

$$\gamma(x,v) = 2\theta'(x)n \tag{13}$$

where n is the normal distance from the wall midline.

Based on the variational energy principle, the total strain energy of the beam is determined by integrating the strain energy density throughout the structural volume. Assuming the material remains isotropic and linearly elastic, the strain energy density U_0 is expressed as:

$$U_0 = \frac{1}{2}\sigma_x\varepsilon_x + \frac{1}{2}\tau\gamma \tag{14}$$

Finally, the strain energy of the beam is:

$$U = \int_\Omega U_0 dV = \frac{1}{2}\int_\Omega \varepsilon_x^L\sigma_x^L + 2\varepsilon_x^N\sigma_x^L + \tau\gamma dAdx \tag{15}$$

Substituting the strain expressions Eqs. (10)-(11) into Eq. (15) and integrating over the cross-section yields:

$$\begin{aligned}U &= \frac{1}{2}\int_L \left(GI_d\theta'^2 + EI_\omega\theta''^2 + EI_y w''^2 + EI_z v''^2\right)dx \\ &+ \frac{1}{2}\int_L \left(2\eta EI_y\Phi'^2 v'' + 2EI_y v'\Phi' w'' - 2EI_z w'\Phi' v''\right)dx\end{aligned} \tag{16}$$

where I_d denotes torsional constant. I_ω is warping constant, I_y and I_z are the moments of inertia.

The external loads are assumed to be applied along the centroidal axis of the beam. Therefore, the work done by the external loads can be obtained as:

$$W = \int_L q_v v + q_w w + \bar{M}_t \theta dx \tag{17}$$

where q_v is the vertical load, q_w is the lateral load. $\overline{M_t}$ is the distributed torque acting on the beam about the shear center.

Substituting the modified torsional moment Eq. (8) into Eq. (19) gives

$$W = \int_L q_v v + q_w w + M_t \theta dx + \int_L q\eta EI_z w'''' + \eta\theta EI_y v''''dx \tag{18}$$

The total potential energy is therefore:

$$\Pi = U - W \tag{19}$$

Applying the stationary condition $\delta\Pi = 0$ leads to the nonlinear equilibrium equations. The vertical bending equation is

$$EI_z v'''' + 2\eta EI_y\left(\theta''^2 + \frac{1}{2}\theta'''' + \theta'\theta'''\right) - \left(EI_y + 2EI_z\right)\theta''w'' - \left(EI_z + EI_y\right)w'''\theta' - EI_z w'\theta''' = q_v \tag{20}$$

The lateral bending equation becomes

$$EI_y w'''' + \left(2EI_y + EI_z\right)v''\theta'' + \left(EI_z + EI_y\right)\theta'v''' + EI_y v'\theta''' = q_w \tag{21}$$

The torsional equilibrium equation is

$$EI_\omega\theta'''' - GI_d\theta'' - 2\eta EI_y\left(v'''\theta' + \frac{1}{2}v'''' + v''\theta''\right) + \left(EI_z - EI_y\right)w''v'' + EI_z w'v''' - EI_y w'''v' = M_t \tag{22}$$

In Eqs. (20)-(22), compared with conventional flexural-torsional formulations, the coupling terms $EI_z\eta\theta''''$ and $EI_z\eta w''''$ explicitly describe the interaction between centroid migration and torsional deformation.

2.4 Nonlinear static equilibrium equation

In engineering practice, the gravity loads transmitted by pipelines are typically introduced to the horizontal channel beam through discrete connection points, with the most unfavorable case occurring when the load is applied at the beam mid-span. Accordingly, the external loading is modeled as a concentrated force acting at ($x=l/2$), where l is the span length of the beam. The corresponding load distribution can therefore be represented by:

$$q_v = F_v\delta(x - x_o), q_w = F_w\delta(x - x_o), M_t = m_t\delta(x - x_o) \tag{23}$$

where q_v and q_w are the concentrated vertical and lateral load amplitudes acting at the beam mid-span, respectively. m_t denotes the externally applied torsional moment at the shear centre, while the total torsional action additionally includes the deformation-induced torsional moment arising from centroid migration; and δ is the Dirac delta function used to represent concentrated actions at the location.

According to the technical specification T/CECS 731-2020 for pipe support and hanger systems, the connections between the horizontal channel beam and the vertical members are idealized as pinned joints. Consequently, the beam is modeled as a simply supported member, and the corresponding kinematic boundary conditions at both ends ((x=0) and (x=l)) can be expressed as

$$v(0) = v(l) = 0, w(0) = w(l) = 0, \theta(0) = \theta(l) = 0 \tag{24}$$

$$v''(0) = v''(l) = 0, w''(0) = w''(l) = 0, \theta''(0) = \theta''(l) = 0 \tag{25}$$

The pinned boundary conditions restrain the transverse displacements of the beam ends in both the vertical and lateral directions, while simultaneously preventing rigid-body torsional rotation at the supports. Such constraints are consistent with the mechanical characteristics of the assembled connections employed in practical prefabricated channel steel hanger systems.

Since the boundary conditions given in Eqs. (24)-(25) are homogeneous, the displacement fields can be approximated using admissible trigonometric functions that satisfy the prescribed end constraints. Accordingly, the vertical displacement ($v(x)$), lateral displacement ($w(x)$), and torsional rotation ($\theta(x)$) are expressed in the form of Fourier sine series as:

$$v(x) = \upsilon_1 \sin(\pi x/l), w(x) = \omega_1 \sin(\pi x/l), \theta(x) = \vartheta_1 \sin(\pi x/l) \tag{26}$$

where υ_1, ω_1, and ϑ_1 are the generalized coordinates corresponding to the first-order vertical bending, lateral bending, and torsional modes, respectively. Owing to the dominance of the fundamental deformation mode under static loading, only the first-order term is retained in the modal expansion.

Substituting Eq. (23) and Eq. (26) into Eqs. (20)-(22) and applying the Galerkin method with sin($\pi x/l$)) as the weighting function, the nonlinear modal equilibrium equations are obtained as follows:

$$EI_z \frac{\pi^4}{2l^3}\upsilon_1 + \eta EI_y \frac{4\pi^3}{3l^3}\vartheta_1^2 - \frac{2\pi^3}{3l^3}\left(EI_y + 2EI_z\right)\vartheta_1\omega_1 + \eta EI_y \frac{\pi^4}{2l^3}\vartheta_1 = F_v \sin\left(\frac{\pi x_0}{l}\right) \tag{27}$$

$$EI_y \frac{\pi^4}{2l^3}\omega_1 + \frac{2\pi^3}{3l^3}\left(2EI_y + EI_z\right)\upsilon_1\vartheta_1 = F_w \sin\left(\frac{\pi x_0}{l}\right) \tag{28}$$

$$\left(EI_\omega \frac{\pi^4}{2l^2} + \frac{l}{2}GI_d\right)\vartheta_1 - \eta EI_y \frac{4\pi^3}{3l^3}\upsilon_1\vartheta_1 + \left(EI_z - EI_y\right)\frac{2\pi^3}{3l^3}\omega_1\upsilon_1 - \eta EI_y \frac{2\pi^4}{l^3}\upsilon_1 = m_t \sin\left(\frac{\pi x_0}{l}\right) \tag{29}$$

Since the peak response of a simply supported beam occurs at mid-span, the generalized coordinates υ_1, ω_1, and ϑ_1 correspond directly to the mid-span vertical displacement, lateral displacement, and torsional rotation, respectively. The resulting modal equilibrium equations incorporate geometric nonlinearity, flexural-torsional coupling, and the additional torsional effect induced by centroid migration, thereby providing a comprehensive description of the large-deformation behavior of prefabricated channel steel hanger beams.

The nonlinear equation system Eqs. (27)-(29) is solved iteratively using the Newton-Raphson method. The converged modal amplitudes are subsequently substituted into Eq. (26) to reconstruct the displacement fields $v(x)$, $w(x)$, and $\theta(x)$.

4. Test specimens

4.1 Stress-strain test

To characterize the mechanical properties of the channel steel used in the prefabricated support

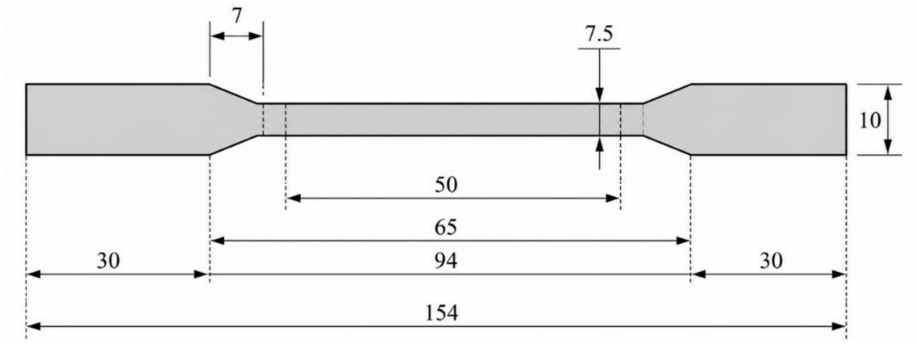

Figure 2. Geometry and dimensions of the tensile specimen

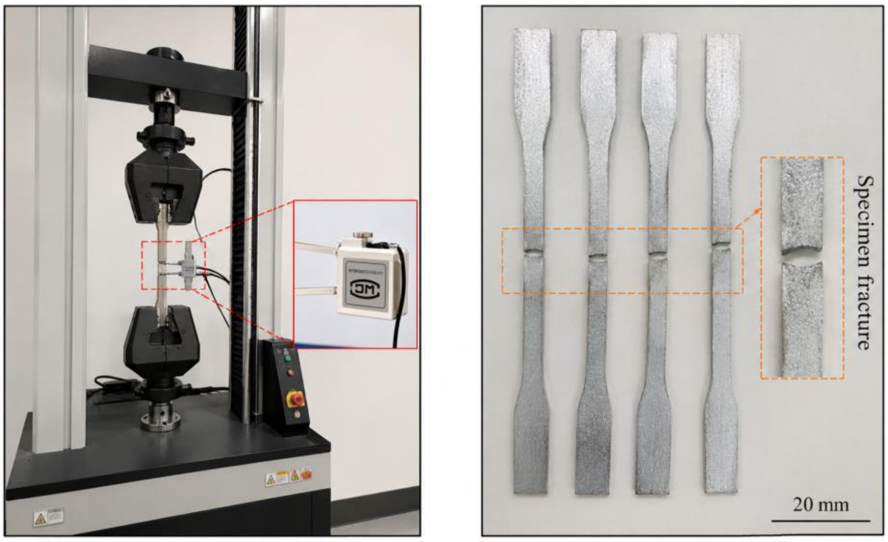

(a) Tensile test machine and extensometer (b) Specimens after testing

Figure 3. Experimental setup for tensile testing and specimens after fracture

and hanger system, room-temperature uniaxial tensile tests were conducted in accordance with ISO 6892-1:2019. The obtained material parameters were subsequently adopted in the theoretical analysis and finite element simulations. Longitudinal tensile specimens were extracted from the channel steel members to determine the elastic modulus, yield strength, and stress-strain relationship. As shown in Fig. 2, the specimens had a gauge length of 50 mm, a width of 12.5 mm, and a thickness of 3.5 mm. Transition fillets were introduced at both ends of the gauge section to reduce stress concentration. Three identical specimens were tested to ensure the repeatability of the measured material properties.

As illustrated in Fig. 3, monotonic tensile tests were performed using a WDW-100 electronic universal testing machine. A 50 mm gauge-length extensometer was attached to the specimen to monitor axial strain. The specimens were carefully aligned and clamped using wedge grips to minimize loading eccentricity. Displacement-controlled loading was adopted, with rates of 2 mm/min and 5 mm/min in the elastic and post-yield stages, respectively. Load, displacement, and strain were recorded automatically throughout the test until fracture.

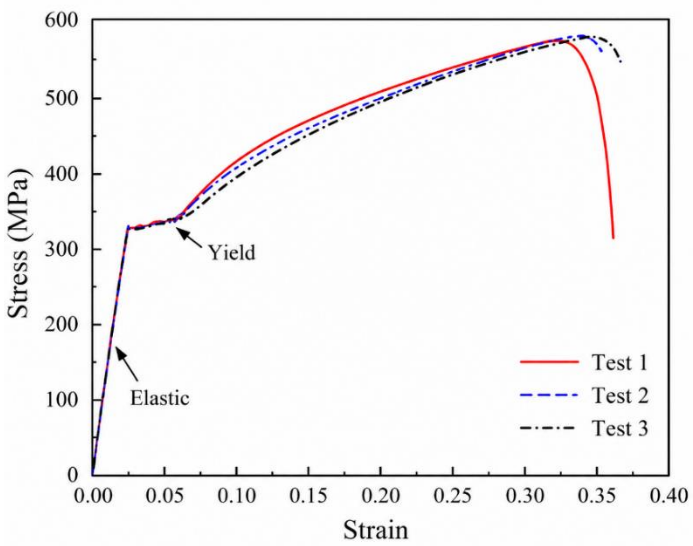

Figure 4. Stress-strain curve of the specimen

Table 1. Geometric parameters of two types of sections

Parameter	C1 Section	C2 Section
I_y	12925.4 mm^4	67353.5 mm^4
I_z	51167.4 mm^4	82083.9 mm^4
I_d	332.05 mm^4	451.687 mm^4
I_ω	7.50×10^6 mm^6	3.77×10^7 mm^6
η	20.52 mm	41.11 mm
G	168.5 GPa	168.5 GPa
l	600 mm	600 mm

As shown in Fig. 4, the stress-strain responses obtained from the three specimens are in close agreement, demonstrating the reliability and repeatability of the tensile tests. The material exhibits an initial linear elastic stage followed by strain hardening and eventual fracture. The elastic modulus was evaluated from the linear elastic region, while the yield strength was determined using the 0.2% offset method. The average elastic modulus and yield strength were found to be 168.5 GPa and 320 MPa, respectively. These values were subsequently used as material parameters in the analytical and finite-element models.

4.2 Experimental verification

Fig. 5 illustrates the test setup adopted to evaluate the flexural-torsional response of prefabricated channel steel hangers. The channel steel beam was connected to the vertical members through hinged joints, forming a simply supported structural system. A concentrated load was applied at the beam mid-span using a loading beam mounted on the testing machine.

Prior to testing, the specimen and loading system were carefully aligned to minimize unintended eccentricity and ensure the proper functioning of the hinged connections.

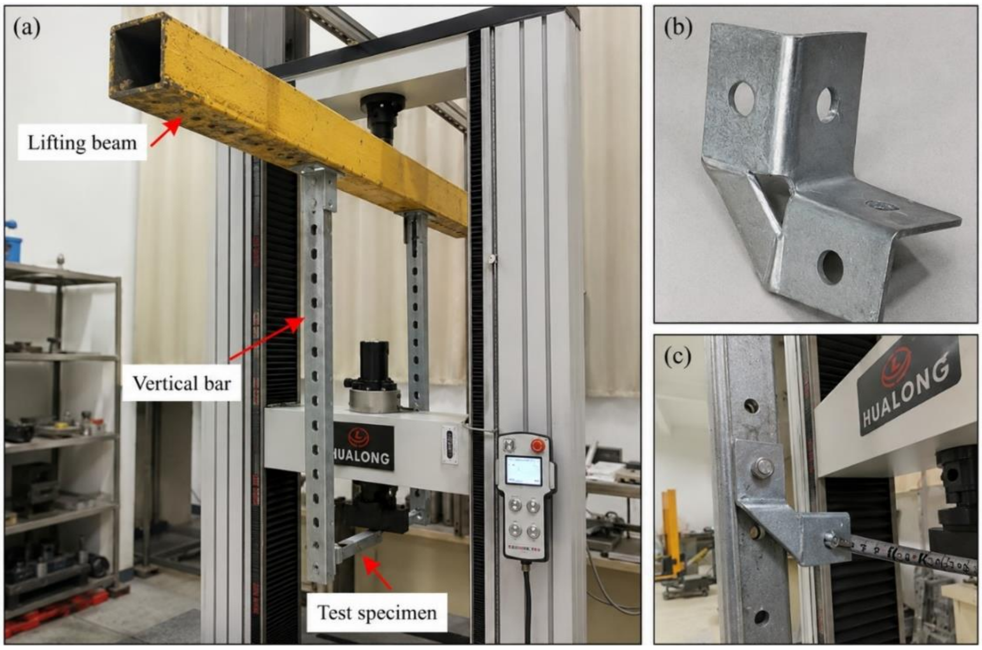

Figure 5. Schematic diagram of experimental setup

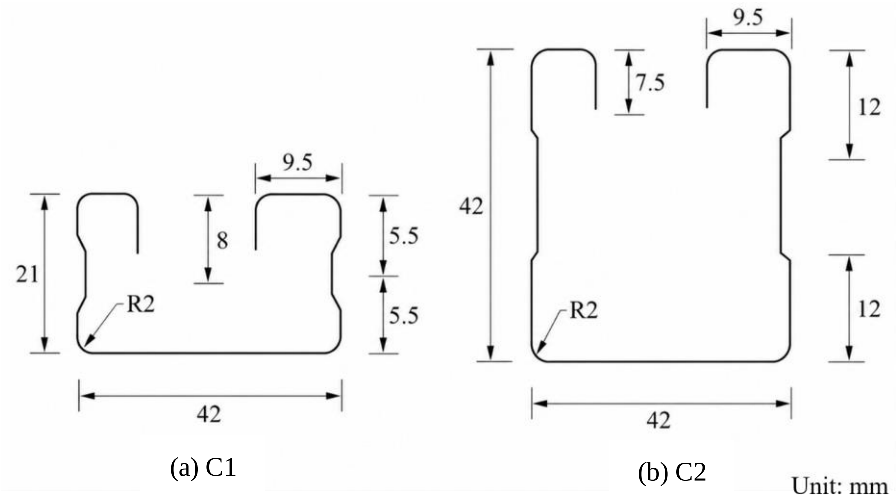

Figure 6. Cross-sectional geometries and dimensions of the channel steel sections

Two representative channel steel sections, C1 and C2 (Fig. 6), were selected as test specimens. Both sections had a uniform thickness of 2 mm, and their geometric and sectional properties are listed in Table 1. These specimens were used to validate the proposed large-deformation flexural-torsional model for different channel steel configurations.

Fig. 7 shows the deformation patterns of the C1 and C2 channel steel beams under mid-span concentrated loading. Both specimens exhibited coupled bending and torsional deformation, which is characteristic of open thin-walled sections. With increasing load, the deformation developed

(a) C1 Section (b) C2 Section

Figure 7. Deformed configuration of the channel steel beam under concentrated loading

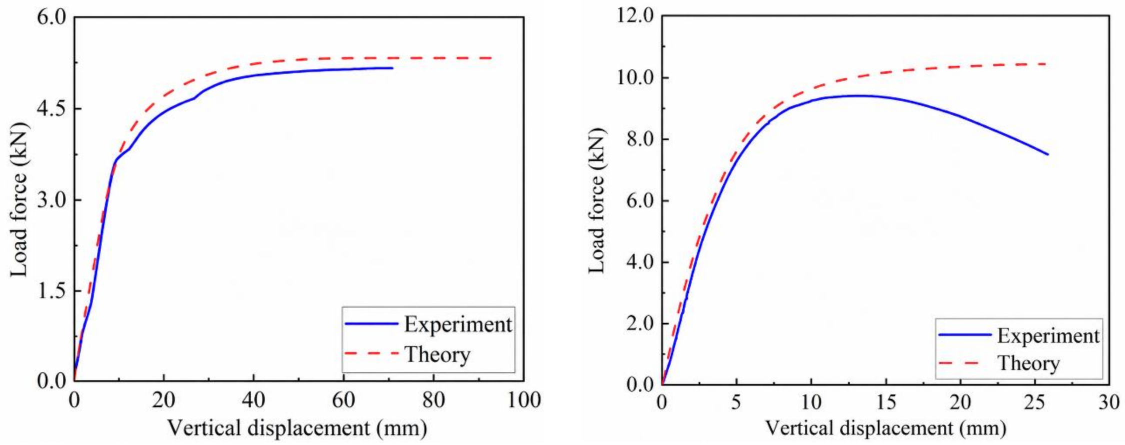

(a) C1 Section (b) C2 Section

Figure 8. Comparison of theoretical and experimental load-midspan displacement curves

progressively and showed a nonlinear trend.

The observed flexural-torsional interaction suggests that torsional effects cannot be neglected in the deformation analysis of prefabricated channel steel hangers. In particular, the increasing torsional response at large deformation levels supports the introduction of geometric nonlinearity and deformation-induced torsional effects in the proposed theoretical model.

The theoretical and experimental mid-span load-displacement curves of C1 and C2 specimens are compared in Fig. 8, with the abscissa as the mid-span vertical displacement and the ordinate as the applied vertical load. The theoretical curves of both specimens are in good agreement with the experimental curves before ultimate load, which fully verifies the correctness and accuracy of the flexural-torsional coupling theoretical model considering large deformation effects. The model can effectively predict the nonlinear load-displacement response of prefabricated channel steel hangers with different cross-sectional geometric parameters under large deformation.

In Fig. 8, a small deviation between the theoretical and experimental curves is observed in the large-deformation stage. Nevertheless, the overall agreement demonstrates the capability of the proposed model to predict the flexural-torsional response of prefabricated channel steel hanger beams.

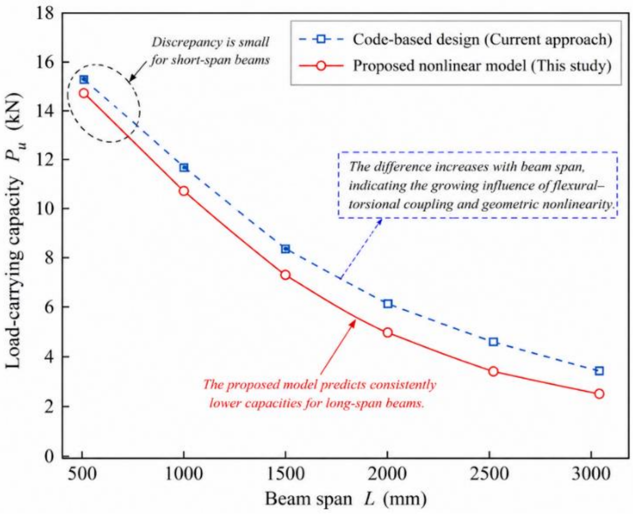

Figure 9. Comparison of load-carrying capacities predicted by the code-based design method and the proposed model

4. Parameter analysis

To further evaluate the applicability of the proposed nonlinear flexural-torsional model, a parametric study was conducted using the validated analytical formulation. The C2 channel steel section was adopted as the reference specimen, and the material properties were taken from the tensile test results. A concentrated load was applied at the beam mid-span, while the beam span was varied from 500 mm to 3000 mm to investigate the influence of structural slenderness on the flexural-torsional response.

Fig. 9 compares the load-carrying capacities predicted by the current code-based design approach and the proposed nonlinear model. For short-span beams, the difference between the two methods is relatively small because the deformation remains limited and the torsional rotation is weak. Under such conditions, the structural response is dominated by bending deformation, and the conventional design method can provide satisfactory predictions. However, the discrepancy increases progressively with beam span. The proposed model consistently predicts lower load-carrying capacities than the code-based approach, indicating that the conventional method tends to overestimate the strength of slender channel steel beams. This difference arises because the current design provisions do not explicitly account for flexural-torsional interaction and geometric nonlinearity.

To quantify the influence of geometric nonlinearity, the nonlinear deformation amplification factor, defined as the ratio of nonlinear displacement to linear displacement, was introduced. As shown in Fig. 10(a), the amplification factor increases from 1.02 to 1.38 when the beam span increases from 500 mm to 3000 mm. This trend demonstrates that geometric nonlinearity becomes increasingly significant as the beam becomes more slender. For short-span beams, the amplification factor remains close to unity, indicating that the linear assumption is generally acceptable. In contrast, for long-span beams, the large vertical deflection alters the structural geometry and introduces additional nonlinear strain components, resulting in a substantial increase in displacement.

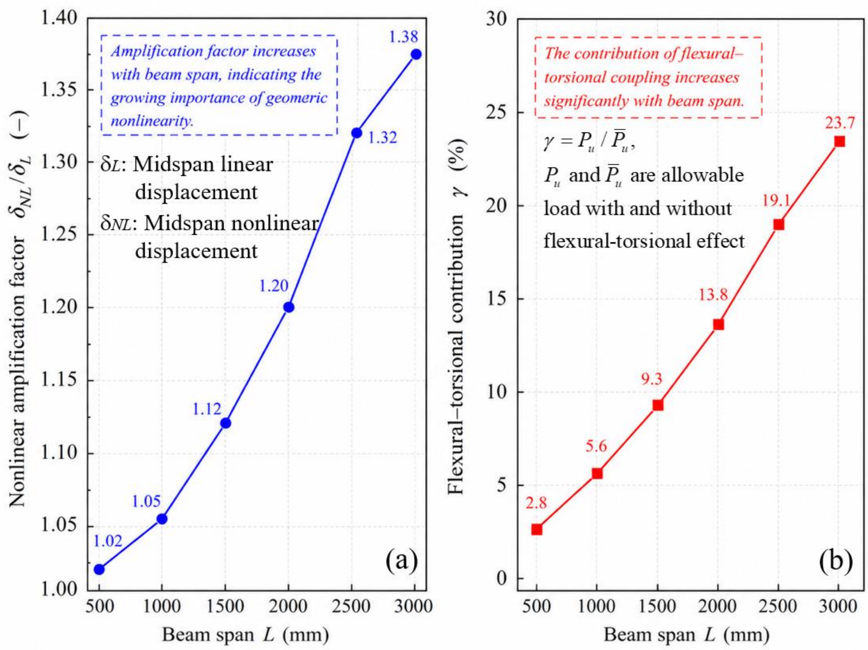

Figure 10. The influence of nonlinear large deformation and Flexural-torsional coupling (a) Variation of nonlinear deformation amplification factor with beam span (b) Contribution of flexural-torsional coupling to total midspan displacement

The contribution of flexural-torsional coupling was further evaluated through the flexural-torsional contribution ratio shown in Fig. 10(b). The contribution increases continuously from 2.8% to 23.7% with increasing beam span. This result indicates that torsional deformation plays only a minor role in short-span beams but becomes an important component of the overall deformation for long-span members. The increase can be attributed to the eccentricity between the centroid and shear centre of the channel steel section. As the beam deflection grows, the induced torsional moment becomes more pronounced, leading to stronger interaction between bending and torsion.

Combining the results of Figs. 9-10, it can be concluded that both geometric nonlinearity and flexural-torsional coupling are span-dependent effects. Their influence is negligible for short-span channel steel hanger beams but becomes increasingly important as the beam span increases. When the span exceeds approximately 2000 mm, the nonlinear amplification factor and flexural-torsional contribution both increase rapidly, suggesting that the conventional linear bending assumption may no longer be adequate. Therefore, the proposed nonlinear flexural-torsional model is particularly necessary for the analysis and design of long-span prefabricated channel steel hanger systems.

5. Conclusions

A nonlinear theoretical and experimental investigation was conducted to evaluate the flexural-torsional behavior of channel steel beams used in prefabricated hanger systems. Based on the analytical derivations, experimental validation, and parametric studies, the following conclusions can be drawn:

- A geometrically nonlinear flexural-torsional model for channel steel beams was developed based on Vlasov thin-walled beam theory and Green-Lagrange strain theory. The model incorporates centroid migration and the resulting additional torsional moment during deformation.
- Experimental results from two representative channel sections showed good agreement with the theoretical predictions. The proposed model accurately captured the nonlinear load-displacement response and flexural-torsional coupling behavior.
- Geometric nonlinearity increased significantly with beam span. The nonlinear deformation amplification factor increased from 1.02 to 1.38 as the span increased from 500 mm to 3000 mm.
- Flexural-torsional coupling became increasingly important for slender beams. Its contribution to the total mid-span displacement increased from 2.8% to 23.7% over the investigated span range.
- Conventional design methods tend to overestimate the load-carrying capacity of long-span channel steel beams because geometric nonlinearity and flexural-torsional interaction are neglected. The proposed model provides a useful tool for the design and safety assessment of prefabricated hanger systems.

References

1. Yilmaz, Y., Ozturk, F., Demir, S. (2024). Buckling behavior of cold-formed steel sigma and lipped channel section beam-columns: experimental and numerical investigation. Journal of Constructional Steel Research, 214. https://doi.org/10.1016/j.jcsr.2024.108456.
2. Peng, Q., Jiao, T., Tang, S., Yan, R., Chen, X., Hu, Y., Liu, C. (2025). A self-sensing variable spring support and hanger for pipeline systems using coaxial-waveguide Fabry–Perot sensing. Measurement, 250, 117186. https://doi.org/10.1016/j.measurement.2025.117186.
3. Shabhari, A., Jeyapragasam, V.V.K., Chandrasekar, D. (2026). Distortional buckling behaviour of web perforated cold-formed steel lipped channel columns. Journal of Constructional Steel Research, 237, 110128. https://doi.org/10.1016/j.jcsr.2025.110128.
4. Torabian, S., Zheng, B., Schafer, B.W. (2015). Experimental response of cold-formed steel lipped channel beam-columns. Thin-Walled Structures, 89, 152-168. https://doi.org/10.1016/j.tws.2014.12.003.
5. Zhang, J.X., Duan, L., Wang, C., Tang, Z., Liu, N., Li, H.T. (2025). DSM design of perforated cold-formed steel lipped channel columns against local, local-distortional and distortional buckling: an experiment-based evaluation. Engineering Structures, 343, 121159. https://doi.org/10.1016/j.engstruct.2025.121159.
6. Yan, J., Young, B. (2002). Column tests of cold-formed steel channels with complex stiffeners. Journal of Structural Engineering, 128(6), 737-745. https://doi.org/10.1061/(ASCE)0733-9445(2002)128:6(737).
7. Oeztuerk, F., Mojtabaei, S.M., Şentürk, M., Pul, S., Hajirasouliha, I. (2022). Buckling behaviour of cold-formed steel sigma and lipped channel beam–column members. Thin-Walled Structures, 173, 108963. https://doi.org/10.1016/j.tws.2022.108963.
8. Liang, D., Fan, S., Gao, S., Liu, M. (2025). The continuous strength method of press-braked lipped channel columns and beams subjected to distortional buckling. Journal of Constructional Steel Research, 235, 109877. https://doi.org/10.1016/j.jcsr.2025.109877.
9. Hasanali, M., Mojtabaei, S.M., Hajirasouliha, I. (2026). Strength prediction of cold-formed steel beam-column channels: data-driven versus prescriptive methods. Journal of Constructional Steel Research,

241, 110295. https://doi.org/10.1016/j.jcsr.2026.110295.
10. Yuan, W.B., Yu, N.T., Li, L.Y. (2017). Distortional buckling of perforated cold-formed steel channel-section beams with circular holes in web. International Journal of Mechanical Sciences, 126, 255-260. https://doi.org/10.1016/j.ijmecsci.2017.04.001.
11. Shabhari, A., Jeyapragasam, V.V.K., Chandrasekar, D. (2024). Local buckling behaviour of web perforated cold-formed steel lipped channel columns. Thin-Walled Structures, 205, 112448. https://doi.org/10.1016/j.tws.2024.112448.
12. Kazmierczyk, F., Zaczynska, M., Kubiak, T. (2025). Lipped channel section laminated beams with non-symmetries subjected to four-point bending. Thin-Walled Structures, 213, 113311. https://doi.org/10.1016/j.tws.2025.113311.
13. das Neves, N.S., Landesmann, A., Camotim, D. (2024). CFS lipped channel beams buckling in distortional modes at elevated temperatures: Behaviour, failure and DSM design. Thin-Walled Structures, 195, 111366. https://doi.org/10.1016/j.tws.2023.111366.
14. Chang, H., Song, X., Qian, Y., Ma, R., Liu, N., Xia, J., Zhang, L. (2023). Experimental investigation of assembly-oriented steel column-beam connection with transverse reverse channels for prefabricated structures. Structures, 56, 104908. https://doi.org/10.1016/j.istruc.2023.104908.
15. Zhou, Y., Hu, B., Gong, Y., Li, Y., Zhang, Y., Lei, M. (2024). Improvement of CSM for high-strength S690 and S960 unlipped channel columns, beams and beam-columns. Structures, 59, 105773. https://doi.org/10.1016/j.istruc.2023.105773.
16. Qi, L., Li, L., Luo, Z., Luo, Z., Jiang, K., Jin, Z. (2025). Shear hysteretic performance of interlocking joints in support and suspension systems. Structures, 80, 110159. https://doi.org/10.1016/j.istruc.2025.110159.
17. Jiang, Z.Q., Niu, Z.Y., Cheng, K.K., Yan, T., Zhang, A.L. (2022). Experimental study of earthquake-resilient high ductility prefabricated opening-web steel channel beam-column joint. Journal of Building Engineering, 49, 104041. https://doi.org/10.1016/j.jobe.2022.104041.
18. Dai, Y., Roy, K., Fang, Z., Chen, B., Raftery, G.M., Lim, J.B. (2022). A novel machine learning model to predict the moment capacity of cold-formed steel channel beams with edge-stiffened and un-stiffened web holes. Journal of Building Engineering, 53, 104592. https://doi.org/10.1016/j.jobe.2022.104592.
19. Qi, L., Meng, R., Shang, Q., Jia, J. (2026). Axial tensile performance of interlocking cross-lap joints in prefabricated hanger systems: Experimental and analytical investigations. Journal of Building Engineering, 115321. https://doi.org/10.1016/j.jobe.2026.115321.
20. Ambrosini, R.D., Riera, J.D., Danesi, R.F. (2000). A modified Vlasov theory for dynamic analysis of thin-walled and variable open section beams. Engineering Structures, 22(8), 890-900. https://doi.org/10.1016/S0141-0296(99)00043-7.
21. Ruocco, E., Minutolo, V. (2015). Buckling analysis of mindlin plates under the green–lagrange strain hypothesis. International Journal of Structural Stability and Dynamics, 15(06), 1450079. https://doi.org/10.1142/S0219455414500795.